FLORE
Repository istituzionale dell'Università degli Studi di Firenze

Impedance spectroscopy characterization of lithium batteries with different ages in second life application

Questa è la Versione finale referata (Post print/Accepted manuscript) della seguente pubblicazione:

Original Citation:

Impedance spectroscopy characterization of lithium batteries with different ages in second life application / Locorotondo E.; Cultrera V.; Pugi L.; Berzi L.; Pasquali M.; Andrenacci N.; Lutzemberger G.; Pierini M.. - ELETTRONICO. - (2020), pp. 1-6. (Intervento presentato al convegno 2020 IEEE International Conference on Environment and Electrical Engineering and 2020 IEEE Industrial and Commercial Power Systems Europe, EEEIC / I and CPS Europe 2020 tenutosi a esp nel 2020) [10.1109/EEEIC/ICPSEurope49358.

Availability:

This version is available at: 2158/1206153 since: 2020-10-08T16:49:50Z

Publisher:

Institute of Electrical and Electronics Engineers Inc.

Published version:

DOI: 10.1109/EEEIC/ICPSEurope49358.2020.9160616

Terms of use:

Open Access

La pubblicazione è resa disponibile sotto le norme e i termini della licenza di deposito, secondo quanto stabilito dalla Policy per l'accesso aperto dell'Università degli Studi di Firenze (https://www.sba.unifi.it/upload/policy-oa-2016-1.pdf)

Publisher copyright claim:

(Article begins on next page)

05 May 2023

Impedance spectroscopy characterization of lithium batteries with different ages in second life application

Edoardo Locorotondo
DIEF
University of Florence
Florence, Italy
edoardo.locorotondo@unifi.it

Vincenzo Cultrera
DINFO
University of Florence
Florence, Italy
vincenzo.cultrera@unifi.it

Luca Pugi
DIEF
University of Florence
Florence, Italy
luca.pugi@unifi.it

Lorenzo Berzi
DIEF
University of Florence
Florence, Italy
lorenzo.berzi@unifi.it

Manlio Pasquali
ENEA
Centro Ricerca ENEA
Rome, Italy
manlio.pasquali@enea.it

Natascia Andrenacci
ENEA
Centro Ricerca ENEA
Rome, Italy
natascia.andrenacci@enea.it

Giovanni Lutzemberger
DESTEC
University of Pisa
Pisa, Italy
lutzemberger@dsea.unipi.it

Marco Pierini
DIEF
University of Florence
Florence, Italy
marco.pierini@unifi.it

***Abstract*— The aging behavior of lithium cell has a profound impact on its performance in terms of energy, power efficiency and capacity fade, especially when it is considered in End of Life (EOL) in automotive field. Lithium battery is considered in EOL if at 85-80% of nominal capacity. Today, the reusing of Electric and Hybrid Vehicles EOL batteries on less-demanding grid connected energy storage applications, giving them a second use/life, is an interesting solution to reduce high potential cost of lithium batteries. Currently, there is a lack of investigation of the performances of these second life batteries. In this paper, authors show the results of the impedance spectroscopy of 20 Ah lithium NMC batteries after EOL, exactly at 100, 85, 80, 60 and 50% of rated capacity, in a wide range of frequency: 450 mHz to 3.5 kHz. By results, there are many way to correlate battery state of health and battery impedance spectroscopy, especially when the battery is in second life.**

Keywords*— *Lithium cell, Impedance spectroscopy, State of health, Second life battery, grid connected energy storage applications, Randles model.

I. INTRODUCTION

Nowadays, battery electric and hybrid vehicles (EVs and HEVs) have a role central to play in Europe's transition from fossil fuels to renewable energy, reducing the greenhouse gas emissions. Lithium batteries, due to high power and energy capability, high efficiency long cycle and calendar life, are established in the automotive market. There is a large scale production and technical improvement for lithium batteries [1][2]. Nevertheless, their high cost is one of the major impediment to increase the market share of EVs and HEVs. Among several solutions, e.g. recycling [3], development of advanced electrode materials and electrolyte solutions [4], the reuse of EV/HEV Li-Ion batteries after their End-Of-Life (EOL), giving them a second life, is one of the major promising solution to decrease the high cost of these batteries today. EV and HEV lithium batteries are considered in EOL if at 85-80% of nominal capacity. Second-life batteries are still expected to be capable of storing, delivering substantial energy and to meet the requirements of a stationary applications. Today, car manufacturers are using the second use option in an attempt to expand their portfolio and enter in the stationary battery market. In cooperation with utility companies, they are launching several battery second life pilot projects. Summary of these projects is presented in [5]. Currently, several studies are focused on the analysis of the economic, technical and environmental matters of battery second life [6][7]. However, there is an increasing need to investigate in depth the potential of using second life batteries for stationary. One of the key challenge related to second life batteries is that the battery behavior and in particular the aging phenomena after first life are not clear known for the different battery chemistries. Therefore, there is a lack of reliable and accurate battery models to assess the applicability of second life batteries into stationary applications. Battery models can be divided in many groups. Electrical models depending on a Thevenin equivalent circuit, adding many R-C groups in series, are usually used, because they solve the trade-off between model complexity and accuracy [8][9]. In literature these models are so-called Electrical Circuit Models (ECMs). However, ECM accurately describes the electrical behavior of the battery while presenting limited physical meaning in its parameters. Instead, many chemical-physical properties of lithium batteries can be observed by Electrochemical Impedance Spectroscopy (EIS) technique [10]. EIS consists of measuring battery impedance in a wide range of frequency. Analyzing several electrochemical battery internal processes with different frequencies, there is the possibility to assess battery SOC [11] in low frequency, internal temperature [12] and SOH [13][14] in high frequency. This paper is focused on the analysis of battery SOH based on EIS measurement at different states of battery ageing and battery SOC. In particular, four different EOL Li-Ion Nickel-Manganese-Cobalt (NMC) batteries with different SOHs will be under test, measuring impedance and analyzing their chemical-physical properties in the following frequency range: 450 mHz to 3.5 kHz. The paper is structured as follows: Section

This project has received funding from the European Union's Horizon 2020 research and innovation program under grant agreement No 769506.

978-1-7281-7455-6/20/$31.00 ©2020 IEEE

II shows the battery EIS and battery modeling in frequency domain, Section III shows laboratory test setup for EIS, tested battery cells with their history, Section IV shows the obtained EIS experimental results, arriving to the conclusions (Section V).

II. Electrochemical Impedance Spectroscopy

A. Theory

The general principle of impedance spectroscopy is to apply a frequency-controlled sinusoidal signal, in current *i*, on the battery. Measuring its voltage response *v*, EIS is performed evaluating the variation of amplitude (or magnitude) and phase shift between battery voltage-current. Considering the battery as a Linear and Time-Invariant (LTI) dynamic system and the exciting current as a stochastic stationary process, battery impedance $\hat{Z}(\omega)$ should be calculated in according to (1), considering $\omega=2\pi f$ the angular frequency [15]:

$$\hat{Z}(\omega)=\frac{\Phi_{vi}(\omega)}{\Phi_{ii}(\omega)} \tag{1}$$

Where $\Phi_{ii}(\omega)$ is the battery input current Power Spectral Density (PSD) and $\Phi_{vi}(\omega)$ is the Cross-PSD (CPSD) between output voltage PSD and input current PSD. Monitoring real $\mathrm{Re}[\hat{Z}(\omega)]$ and imaginary $\mathrm{Im}[\hat{Z}(\omega)]$ part of the estimated impedance, its magnitude and phase shift are evaluated for each frequency ω. In this paper, authors use broadband input current excitation signal, in particular, Pseudo Random Binary Sequence (PRBS) signals. The main advantage of this signal is its flat PSD in at least one decade of frequency range. Thus, exciting battery with PRBS current signal, it is possible to estimate battery impedance in a wide frequency range with less energy consumption and test time, finally validating the previous assumption of battery system as LTI. More details about theory and simulation results of this fast identification method are shown in [16].

B. Battery modeling

Usually, EIS results are presented in Nyquist diagram, comparing real impedance values with the negative of the imaginary impedance values, because lithium batteries showed ohmic-capacitive feature in the major part of interested frequency range. Fig.1 shows the general shape of battery impedance in Nyquist diagram. It presents five different well identifiable dynamic internal processes which occur simultaneously during battery operation. Concerning battery EIS analysis, electrical Randles circuit models are usually used to reproduce similar Nyquist diagrams [17]. There are many circuit configurations in [18]. Fig.1 shows the Randles circuit model adopted in our study. This circuit introduces Constant Phase Elements (CPE), which improve the match between the fit and the experimental battery EIS measurement in frequency. Its transfer function is described by (2):

$$Z_{CPE}(\omega)=\frac{1}{(j\omega)^{\alpha}Q_W} \tag{2}$$

CPE describes partially a capacitive behavior. It includes two parameters: capacitance Q and α, where $\alpha \in [0,1]$. This last parameter is called depression factor. Usually CPE is used in parallel with a resistance R in order to present in Nyquist diagram semi-ellipses arcs, which are common features for impedance in the battery electrode/electrolyte [19]. In a parallel R-CPE configuration, transfer function is described in according to (3):

$$Z_{R//CPE}=\frac{R}{1+\tau(j\omega)^{\alpha}} \tag{3}$$

Where $\tau = QR$. It's noticeable that the impedance (3) for α equal to 1, describes an ideal RC component, represented in Nyquist diagram by a semi-circumference, while for α=0 (3) represents a static resistance. More details about CPE are reported in [18]. As mentioned previously, CPE will be used in the circuit configuration adopted for battery EIS description, and the parameters are as follows presented in relation to Fig.1.

- **Ohmic and connectors impedance (R_Ω, L):** At the highest frequency, an inductive behavior L is observed due to reactance of battery connectors. At zero-crossing frequency, Ohmic resistance R_Ω is evaluated. The current delivered/supplied by the battery comes with voltage drop due to current collectors, active material, electrolyte and separator [10], represented by R_Ω .
- **SEI film (R_{SEI}, CPE_{SEI}):** The first semi-ellipses is associated with the growth of the so-called Solid-Electrolyte-Interphase (SEI) film on the electrode negative surface. During cycling, partial decomposition of the active material at the electrolyte surface is observed, creating a solid layer between anode and electrolyte [19], causing an increase of battery internal resistance R_{SEI} . Usually, a R_{SEI}, CPE_{SEI} branch is used to model this phenomenon.
- **Charge transfer phenomena and double layer capacitance (R_{CT}, CPE_{DL}):** The second semi-ellipses is associated to the charge transfer resistance R_{CT} and double layer capacity CPE_{DL} . The first parameter corresponds to the resistance in the charge transfer between electrodes and is often attributed to the Butler-Volmer kinetics of the reaction [11][17]. The double layer capacitance is the electrical representation of the electrode-electrolyte interface, which is proportional to this area [19].
- **Diffusion process (CPE_W):** at lowest frequency, it is noticeable the damping effect on the electroactive species related to the mass transport [19] that modifies the electrochemical potential. The most common parameter for modeling diffusion behavior is the Warburg impedance. In this work, we consider the infinite Warburg element transfer function, which is equal to (3), fixing the depression factor α to 0.5 (in Nyquist diagram it means a bisector):

$$CPE_W(\omega) = \frac{1}{\sqrt{(j\omega)}Q_W} \tag{4}$$

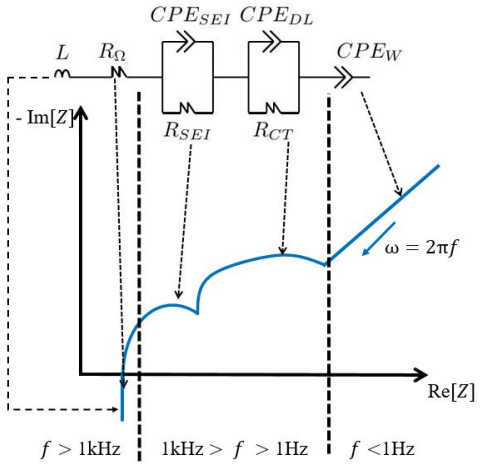

Fig. 1. Reference spectrum of Li-Ion cell in a wide frequency range and battery EIS modeling.

Thus the complete battery impedance transfer function presented in this work is in according to (2)-(4):

$$Z_{\text{model}}(\omega) = j\omega L + R_\Omega + \frac{R_{SEI}}{1+(j\omega)^{\alpha_{SEI}}\tau_{SEI}} + \frac{R_{CT}}{1+(j\omega)^{\alpha_{DL}}\tau_{CT,DL}} + \frac{1}{\sqrt{j\omega}Q_W} \tag{5}$$

C. Electrical Randles circuit model identification

From experimental EIS data Z_{meas} obtained in a defined frequency range $f \in [f_{low}, f_{high}]$, authors define the parameter identification by the battery impedance model in according to (5). This model is Non Linear in the Parameters (NLIP). In this paper, the parameters $\beta = [L, R_\Omega, R_{CT}, Q_{DL}, \alpha_{DL}, R_{SEI}, Q_{SEI}, \alpha_{SEI}, Q_W]$ are identified so that battery impedance model (5) best fit the experimental data, minimizing the following sum of square prediction error:

$$\arg\min_{\beta} \left[\sum_{f=f_{low}}^{f_{high}} (\text{Re}[Z_{meas}(2\pi f)] - \text{Re}[Z_{\text{model}}(2\pi f)])^2 \sum_{f=f_{low}}^{f_{high}} (\text{Im}[Z_{meas}(2\pi f)] - \text{Im}[Z_{\text{model}}(2\pi f)])^2 \right] \tag{6}$$

The solution of the identification of the NLIP model, that minimizes (6), should be solved using the Levenberg-Marquardt algorithm (LMA). The LMA finds only local minimum, so it requires an accurate choice of the initial parameter vector β (Table I).

TABLE I. INITIAL MODEL PARAMETER VALUES USED FOR BATTERY IMPEDANCE IDENTIFICATION

Parameters	Numeric Values	Unit
L	10^{-8}	H
R_Ω	10^{-2}	Ω
R_{SEI}	10^{-2}	Ω
Q_{SEI}	1	F
α_{SEI}	0.5	/
R_{CT}	10^{-2}	Ω
Q_{DL}	10	F
α_{DL}	0.5	/
Q_W	1000	kF
α_W	0.5 (fixed)	/

III. EXPERIMENT DESCRIPTION

A. Battery cell under test

The battery under test is a Li-Ion NMC Cathode pouch cell type, having a nominal capacity of 20 Ah. The EIS test is performed on five cells of the same manufacturer [20], but at different State of Health (SOH). In this paper, battery SOH is considered by the variation of battery capacity compared to its ideal condition, in this case, 20 Ah. Current battery SOH is defined in Table II. It's noticeable that battery n. #3-#8 should be considered in automotive field as in EOL, therefore, ready for possible second life use.

TABLE II. BATTERY CELL SOH

Battery no.	Capacity evaluated	State of Health
#0	20Ah	100%
#3	16Ah	80%
#4	17Ah	85%
#5	12Ah	60%
#8	10Ah	50%

The EOL cells (#3-#8) were subjected to 4 different cycle life test, composed by constant-current (CC) and, finally, constant-voltage (CV) charging (0.5C, where C is nominal capacity); followed by discharging phases, interspersed with pauses, at a room temperature of 35°C [21]. A summary of these cycle life test is presented in Table III. Cycle life tests were carried out in ENEA research center [21] from 2015 to 2017. More details about these tests are given in [21][22]. Afterwards, the cells have not been used for about 2 years, and have been storage in the same conditions (in a not thermally controlled environment). Finally, after few preconditioning cycles, cell capacity are evaluated and shown in Table II.

TABLE III. CYCLE LIFE TEST

Battery no.	Discharge C-Rate	Depth of Discharge	Performed cycle number	Last capacity estimated
#3	3	80-20%	2550	15.14 Ah
#4	5	80-20%	2000	15.09 Ah
#5	1	90-10%	2400	12.91 Ah
#8	3	90-10%	1600	15.48 Ah

B. Laboratory Test setup

All the EIS measurement are performed with the lab test setup shown in Fig.2. Firstly, battery is excited in current using the PRBS signal, generated by the low-cost programmable hardware presented in [23], in the frequency range from 450 mHz to 3.5 kHz. Current amplitude of excited PRBS signal is selected in relation to the capacity of the cell under test: this value was assessed in order to maintain the battery SOC

variation and the internal temperature excursion very low [10], but maintaining the SNR between measured signal and noise high [16], thus ensuring good accuracy and that the battery system could be considered as LTI system. In this work, current amplitude value is equivalent to 0.3C, where C is the current battery capacity. The DSpace MicroLabBox DS1202 has been used as battery voltage, current and temperature data measurement and acquisition, with a sample time of 20 kHz.

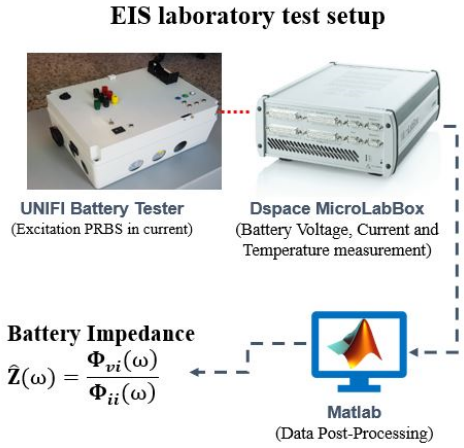

Fig. 2. Laboratory test & measurement setup.

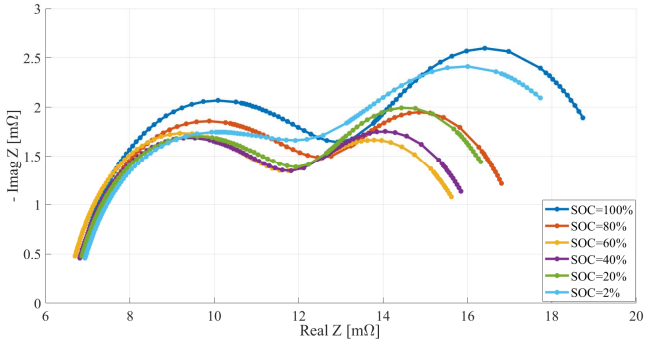

Fig. 3. Measured battery impedance results on cell #5 (SOH 60%) at different SOC.

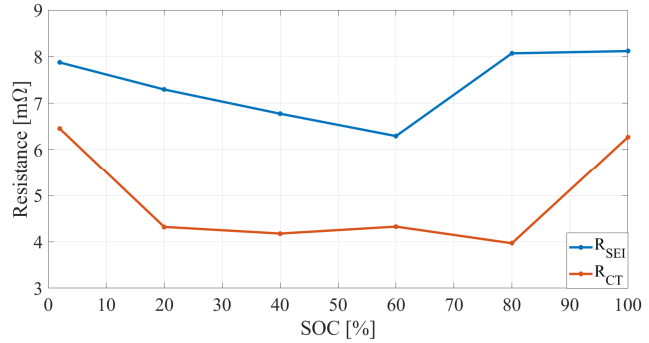

Fig. 4. Dependence of battery SEI resistance and charge-transfer resistance (R_{SEI}, R_{CT}) at different SOC (cell #5, SOH=60%).

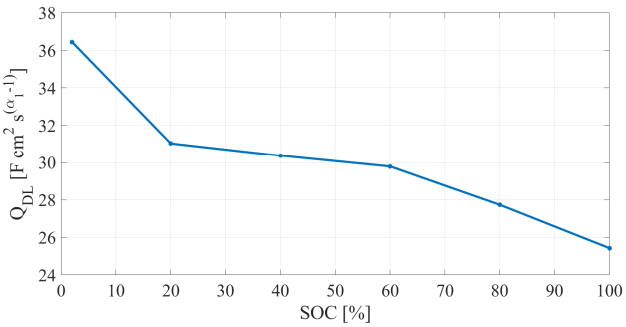

Fig. 5. Dependence of battery double layer capacitance at different SOC (cell #5, SOH=60%).

IV. Results

A. Analysis of battery EIS results at various SOC

In this subsection, the relationship between battery impedance spectra with battery SOC is discussed. EIS test are performed on NMC cells with lab-test setup shown in Fig.2 (more details in [23]), using PRBS excitation signal [16]. Every EIS test is performed with a SOC variation less than 2% and without temperature variation, thus working in the fixed operating condition. In Fig.3 the evaluated impedance spectra for the cell with SOH 60% are shown for 6 different battery SOC. The shape of the impedance is similar for all the SOC values. In particular, many considerations should be highlighted at low frequency: it's noticeable that the amplitude of the semi-ellipses becomes very high at the extreme part of the battery SOC window (2%, 100%). In particular, the amplitude of the second semi-ellipse (defined by the R_{CT}, CPE_{DL}) increases, revealing an increase of charge-transfer resistance, as shown in Fig.4, similar to other cell chemistries [12][24]. Moreover, in Fig.4, the increase of the R_{SEI} is observed, whose value was smaller than R_{CT} when the cell was in the begin of life [25]. Finally, the double layer capacitance increases, when battery SOC is decreasing, as shown in Fig.5.

B. Dependence of battery EIS results at various SOH

As mentioned in the introduction, EIS analysis allows us to extrapolate much information about current battery chemical-physical properties and battery SOH. Fig.6 shows the results of evaluated battery impedance spectra on the cells under test at fixed SOC=60%. It's noticeable that a decrease of battery SOH, so a battery degradation, implies a shift to the right of the impedance spectra in the Nyquist diagram with respect to the real impedance axes. This behavior corresponds to an increase of the ohmic resistance R_{Ω} proportional to the battery capacity degradation, as it happens in its first life [13][14][25]. Moreover, an increase of the two semi-ellipses arcs are noticeable, in according to [11][12], more noticeable as SOH decreases. In particular, the length of the two ellipses semi-axes approximately corresponds to the sum of the SEI and charge-transfer resistance (R_{SEI}, R_{ct}) [18], so an increase of ellipses semi-axes corresponds to the increase of (R_{SEI}, R_{ct}) over battery lifetime. This phenomenon is present also in the first life of the battery [25], but becomes more evident in the second life, especially for the increasing of R_{SEI}. Since the aging effects are difficult to evaluate directly

from impedance spectra, further investigations of the behavior of model parameters (5) are necessary. Given impedance spectra and using Levenberg-Marquardt algorithm, battery impedance model parameters are estimated in according to (6) and are presented in the Fig.7,8 for second life batteries.

Fig.7 shows that the ohmic, SEI and charge-transfer resistance linearly increase during battery aging process [25][26], especially R_Ω, R_{SEI} during battery second life. As already mentioned, R_{SEI} and R_{CT} increase at the two extreme windows of battery SOC, while ohmic resistance R_Ω remain constant. Concerning second life, one of the more efficient indicator of the battery SOH is the increase of the sum R_{SEI} + R_{CT}, which value is approximately obtained as the sum of the two semi-ellipses semi-axes length. In order to obtain a complete representation of these semi-ellipses, authors suggest to measure impedance spectra at least in two decades of frequency range: from 1Hz to 1kHz. This frequency range is only indicative for this kind of cell. Finally, Fig.8 shows a decrease of battery double layer capacitance represented by the CPE (Q_{DL}, α_{DL}), which shows also a linear trend respect to battery SOC. This result does not agree with [26] and partially agrees with [14]. This is probably because it is difficult to evaluate the Q_{DL} parameter directly by impedance spectra without using a non-linear parameter identification method with experimentally measured impedance data in a wide frequency range (at least from 2 mHz to 5 kHz [26]).

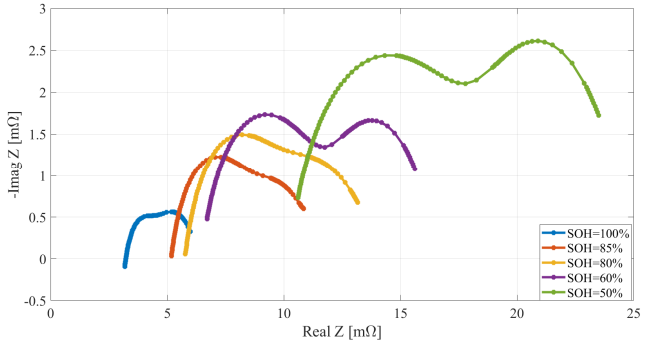

Fig. 6. Measured battery impedance results on NMC cells with different SOH, at fixed battery SOC=60%.

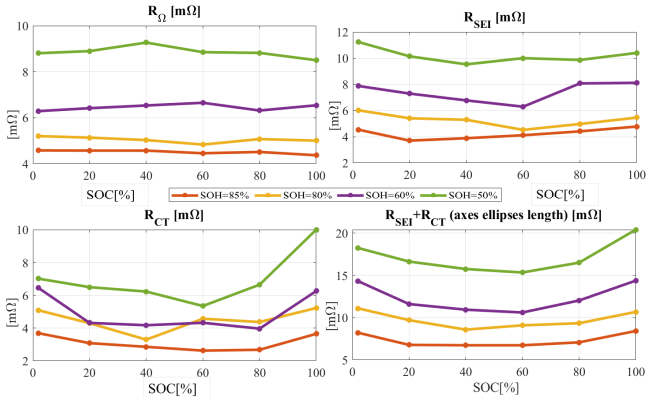

Fig. 7. Model resistance parameters extraction on NMC cells with different SOH.

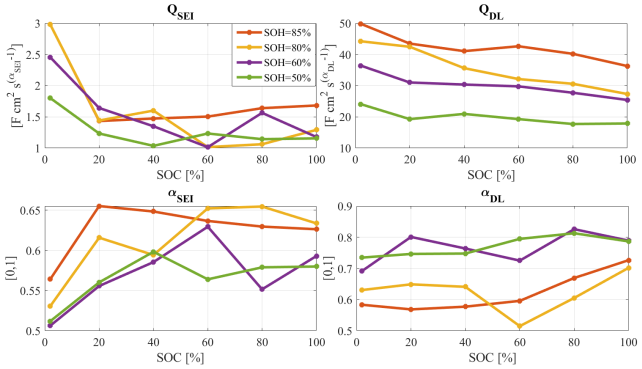

Fig. 8. Model constant phase element parameters extraction on NMC cells with different SOH.

V. Conclusions

This paper has investigated on the lithium battery performance in EOL, for second life application, through EIS, validating the suitability of this technique to diagnose battery degradation.

To this scope, five 20 Ah NMC cells, one considered as new, and other four in EOL, were tested, measuring EIS for frequency range 450 mHz to 3.5 kHz at different SOCs.

The influence of aging on the batteries has been investigated with the parametrization of battery impedance circuit model based on Randles circuit, by experimental impedance data.

Results indicate that the parameters Q_{DL}, R_{SEI}, R_{CT} vary with battery SOC. However, Q_{DL} is difficult to directly evaluate, and, although R_{SEI}, R_{CT} are simply to identify by impedance spectra, their value change majorly only at the extreme of SOC window. Thus battery EIS should be not considered as a valuable method to identify battery SOC.

Instead, resistance parameters R_Ω, R_{SEI}, R_{CT} increase with the battery degradation. In particular, battery SOH is well identifiable, especially in second life, by the length of the ellipses semi-axes (R_{SEI} + R_{CT}), which value should be simple to evaluate.

Acknowledgment

The present work is using battery cells coming from the ENEA research center and the University of Pisa. Authors wish to thank all for their support and collaboration. All the activities reported in this paper were carried out within the Smart Energy Lab of the University of Florence.

References

[1] Berckmans, G., Messagie, M., Smekens, J., Omar, N., Vanhaverbeke, L., & Van Mierlo, J. (2017). Cost projection of state of the art lithium-ion batteries for electric vehicles up to 2030. Energies, 10(9), 1314.

[2] Blomgren, G. E. (2016). The development and future of lithium ion batteries. Journal of The Electrochemical Society, 164(1), A5019.

[3] Huang, B., Pan, Z., Su, X., & An, L. (2018). Recycling of lithium-ion batteries: Recent advances and perspectives. Journal of Power Sources, 399, 274-286.

[4] Marom, R., Amalraj, S. F., Leifer, N., Jacob, D., & Aurbach, D. (2011). A review of advanced and practical lithium battery materials. Journal of Materials Chemistry, 21(27), 9938-9954.

[5] Bobba, S., Podias, A., Di Persio, F., Messagie, M., Tecchio, P., Cusenza, M. A., ... & Pfrang, A. (2018). Sustainability Assessment of Second Life Application of Automotive Batteries (SASLAB). JRC Exploratory Research (2016-2017), Final report.

[6] Martinez-Laserna, E., Gandiaga, I., Sarasketa-Zabala, E., Badeda, J., Stroe, D. I., Swierczynski, M., & Goikoetxea, A. (2018). Battery second life: Hype, hope or reality? A critical review of the state of the art. Renewable and Sustainable Energy Reviews, 93, 701-718.

[7] Neubauer, J., & Pesaran, A. (2011). The ability of battery second use strategies to impact plug-in electric vehicle prices and serve utility energy storage applications. Journal of Power Sources, 196(23), 10351-10358.

[8] Huria, T., Ludovici, G., & Lutzemberger, G. (2014). State of charge estimation of high power lithium iron phosphate cells. Journal of Power Sources, 249, 92-102.

[9] Locorotondo, E., Pugi, L., Berzi, L., Pierini, M., & Pretto, A. (2018, June). Online State of Health Estimation of Lithium-Ion Batteries Based on Improved Ampere-Count Method. In 2018 IEEE International Conference on Environment and Electrical Engineering and 2018 IEEE Industrial and Commercial Power Systems Europe (EEEIC/I&CPS Europe) (pp. 1-6). IEEE.

[10] Andre, D., Meiler, M., Steiner, K., Wimmer, C., Soczka-Guth, T., & Sauer, D. U. (2011). Characterization of high-power lithium-ion batteries by electrochemical impedance spectroscopy. I. Experimental investigation. Journal of Power Sources, 196(12), 5334-5341.

[11] Andre, D., Meiler, M., Steiner, K., Walz, H., Soczka-Guth, T., & Sauer, D. U. (2011). Characterization of high-power lithium-ion batteries by electrochemical impedance spectroscopy. II: Modelling. Journal of Power Sources, 196(12), 5349-5356.

[12] L.H.J. Raijmakers, D.L. Danilov, J.P.M. van Lammeren, M.J.G. Lammers, P.H.L. Notten, "Sensorless battery temperature measurements based on electrochemical impedance spectroscopy," Journal of Power Sources, vol. 247, pp. 539-544, 2014.

[13] De Sutter, L., Firouz, Y., De Hoog, J., Omar, N., & Van Mierlo, J. (2019). Battery aging assessment and parametric study of lithium-ion batteries by means of a fractional differential model. Electrochimica Acta, 305, 24-36.

[14] Stroe, D. I., Swierczynski, M., Stan, A. I., Knap, V., Teodorescu, R., & Andreasen, S. J. (2014, September). Diagnosis of lithium-ion batteries state-of-health based on electrochemical impedance spectroscopy technique. In 2014 IEEE Energy Conversion Congress and Exposition (ECCE) (pp. 4576-4582). IEEE.

[15] L. Ljung, "System Identification - Theory for the User", Prentice Hall, 1999.

[16] E. Locorotondo, S. Scavuzzo, L. Pugi, A. Ferraris, L. Berzi, A. Airale, M. Pierini, M. Carello, Electrochemical Impedance Spectroscopy of Li-Ion battery on-board the Electric Vehicles based on Fast nonparametric identification method, 2019 IEEE International Conference onEnvironment andElectricalEngineeringand2019IEEE Industrial and Commercial Power Systems Europe (EEEIC/I&CPS Europe), IEEE, 2019, pp. 1–6, IEEE.

[17] Randles, J. E. B. (1947). Kinetics of rapid electrode reactions. Discussions of the faraday society, 1, 11-19.

[18] F. Berthier, J.P Diard, R. Michel, "Distinguishability of equivalent circuits containing CPEs: Part I. Theoretical part." Journal of Electroanalytical Chemistry, 510(1-2), 1-11, 2001.

[19] Al-Nazer, R., Cattin, V., Granjon, P., & Montaru, M. (2012, June). A new optimization algorithm for a Li-Ion battery equivalent electrical circuit identification.

[20] EIG battery official site, www.eigbattery.com.

[21] Andrenacci, N., & Sglavo, V. (2017). Stato dell'arte dei modelli di invecchiamento per le celle litio-ione. Applicazione al caso di studio delle celle NMC invecchiate in ENEA. Report RDS/PAR2016/163.

[22] Ceraolo, M., Giglioli, R., Lutzemberger, G., Langroudi, M. M., Poli, D., Andrenacci, N., & Pasquali, M. (2018, June). Experimental analysis of NMC lithium cells aging for second life applications. In 2018 IEEE International Conference on Environment and Electrical Engineering and 2018 IEEE Industrial and Commercial Power Systems Europe (EEEIC/I&CPS Europe) (pp. 1-6). IEEE.

[23] Serni, T., Locorotondo, E., Pugi, L., Berzi, L., Pierini, M., Cultrera, V., A Low Cost Programmable Hardware for Online Spectroscopy of Lithium Batteries. In 2020 IEEE Mediterranean Eletrotechnical Conference (MELECON) (pp. 1-6), Palermo, under review.

[24] Samadani, E., Farhad, S., Scott, W., Mastali, M., Gimenez, L. E., Fowler, M., & Fraser, R. A. (2015). Empirical modeling of lithium-ion batteries based on electrochemical impedance spectroscopy tests. Electrochimica acta, 160, 169-177.

[25] Olofsson, Y., Groot, J., Katrašnik, T., & Tavčar, G. (2014, December). Impedance spectroscopy characterisation of automotive NMC/graphite Li-ion cells aged with realistic PHEV load profile. In 2014 IEEE International Electric Vehicle Conference (IEVC) (pp. 1-6). IEEE.

[26] Waag, W., Käbitz, S., & Sauer, D. U. (2013). Experimental investigation of the lithium-ion battery impedance characteristic at various conditions and aging states and its influence on the application. Applied energy, 102, 885-897.